ISSN: 2663-2187

https://doi.org/10.48047/AFJBS.6.10.2024.6120-6137

Temperature Effect on Decolorization of Water Using $ZnCl_2$-Activated Biomaterial

CHERGUI Yamina[1]; OUAZANI Fouzia[2]; BENKHATOU Soumia[3]; IDDOU Abdelkader[4]

[1] *Laboratoiry of Saharan Natural Resources (LSNR), University of Ahmed draia Adrar, Algeria*

[2] *Laboratory of Process Engineering, Materials and Environment, Faculty of Technology, University of Djillali Liabes, PO Box 89, Sidi Bel Abbes 22000 -Algeria.*

[3] *Laboratoiry of Materials Application at Environment, Sciences and Technologies faculty, University of Mascara, BP305 street of Mamounia, 29000 Mascara, Algeria*

[4] *Higher School of Saharan Agriculture – Adrar, Algeria*

Email: chergui.amina@yahoo.fr

Article History
Volume 6, Issue 10, 2024
Received:18 Apr 2024
Accepted:20 Jun 2024
doi: 10.48047/AFJBS.6.10.2024.6120-6137

Abstract

Water pollution caused by organic substances such as dyes necessitates the implementation of advanced treatment processes. Among the proposed solutions, using adsorption techniques with cost-effective adsorbent materials derived from plant waste has been suggested. The aim of this study is to assess the effectiveness of activated carbon in adsorbing Rhodamine B. The research investigates the adsorption mechanism of Rhodamine B, focusing on parameters including pH, adsorbent mass, and initial dye concentration. The obtained results were analyzed using kinetic models such as pseudo-first order, pseudo-second order, Elovich, and intraparticle diffusion equations. The findings demonstrate that the adsorption kinetics of Rhodamine B on the chemically and physically activated biomaterial conform well to the pseudo-second order model, with correlation coefficients (R^2) ≥ 1 at all tested temperatures. Intraparticle diffusion is identified as the controlling step in the adsorption process after 50 minutes of contact time. Moreover, thermodynamic analysis and adsorption isotherms indicate that the adsorption process is favorable, spontaneous, and exothermic.

Keywords: Adsorption, Pseudo-second-order model, Activated carbon, Rhodamine B.

1. INTRODUCTION

Water is an essential element in our lives. Consequently, water pollution poses the most dreadful danger to humanity since its appearance on Earth. Various pollutants alter the quality of water, including dyes, which are widely used in several sectors such as food, textile, and paint industries (**Choyk KH et al., 1999**). Some of these dyes are highly toxic, thus posing a threat to the environment (**Faria PPC et al., 2004**). This situation prompts environmental preservation and protection services to periodically monitor industrial and domestic discharges to intervene as necessary. Over the years, numerous methods have been developed for treating water polluted by dyes. It turns out that adsorption is one of the most effective methods (simple and less costly technology) (**Gomez V et al., 2007**). The major advantage of this technique is its ability to use a wide variety of adsorbents (clays, activated carbons, zeolites, etc.). According to several studies, adsorption on activated carbon yields good results (**Kennedy LJ et al., 2007, Kannan N et al., 2002**).

The adsorption properties of activated carbons, determined by their porosities and specific surface areas, find applications in various liquid and gas phase processes. Liquid-phase applications include the treatment of drinking water, groundwater remediation, and decolorization.

In recent years, activated carbons synthesized from agricultural residues have been extensively utilized as adsorbents to treat colored effluents due to their highly porous structure, large specific surface area, and high adsorption capacity (**Pearce CI et al., 2003, Mc Mullan G et al., 2001**).

This study investigates the adsorption of the Rhodamine B dye onto activated carbon prepared from a biomaterial activated by $ZnCl_2$. Various parameters, such as pH, adsorbate mass, stirring speed, and contact time at different temperatures, are considered.

Particular attention is given to examining the equilibria related to the kinetics and thermodynamics of adsorption to predict the mode of fixation.

2. Experimental Setup and Procedures

2.1 adsorbent and adsorbat

With the aim of valorizing plant-based biomass, considered as waste from the Algerian wine industry, referred to as "Grape Marc," the raw grape marc was air-dried before being crushed and sieved to extract the particle fraction between 500 and 1000 µm. It was then washed and dried at 110 °C for 24 hours.

A solution of zinc chloride ($ZnCl_2$) was used to activate the obtained carbons. The resulting material was washed with a 0.1N hydrochloric acid (HCl) solution, then filtered, rinsed with distilled water several times, and dried in an oven at 110°C for 24 hours.

This biomaterial, after chemical and thermal activation (MRA), was tested for the removal of a basic dye: Rhodamine B. The removal was carried out from aqueous solutions in batch mode.

Rhodamine B, the model compound of this study, is a basic dye from the xanthene class. It is presented in the form of dark green crystals **(Makhlouf M et al., 2013)**. **Fig.1** illustrates its molecular structure. A stock solution of 1000 mg/L was prepared by dissolving 2 g of dye in distilled water. The colored solutions of different concentrations used in this study were prepared by diluting the stock solution with distilled water.

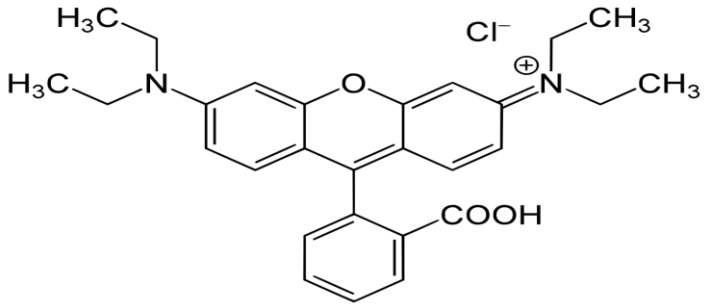

Fig.1 ***Molecular structure of Rhodamine B***

2.2 Experimental Setup

2.2.1 FTIR analysis

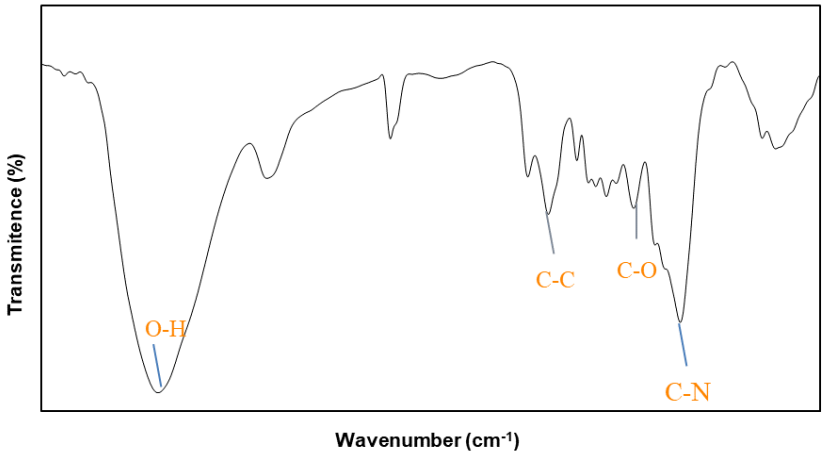

Fig.2 ***FTIR of MRA***

Infrared (IR) spectroscopy is an important technique used for the identification of characteristic functional groups on the adsorbent surface. These groups are often responsible for adsorbent-adsorbate bonds. **(Kushwaha A.K et al., 2014)**

The infrared spectra of the material used is shown in Figure 2. The broad absorption band between 3400–3375 cm^{-1} corresponds to the hydrogen stretching vibrations of the O-H hydroxyl groups (carboxyls, phenols or alcohols) and adsorbed water **(Liou T-H., 2010)**. It also corresponds to the O-H elongation vibration of cellulose, pectin and lignin **(Djilani C et al., 2012)**. Between 2916 and 2875 cm^{-1} the bands of stretching vibrations which correspond to the asymmetric and symmetrical C–H stretching vibrations of the lateral alkyl chains **(Sych N.V et al., 2012)**. These bands decreased in intensity upon activation with $ZnCl_2$, indicating the increase in aromaticity of the carbons. **(Spagnoli A.A et al., 2017)**

The appearance of bands around 1700 cm^{-1} for activated materials, which are attributed to the stretching vibrations of the C=O groups of ketones, aldehydes, lactones or carboxylic groups, the spectra also show a band between 1650 and 1550 cm^{-1}, due to the stretching vibrations of the C=C bonds of the olefinic structure, and correspond to the stretching vibrations of the C-C aromatic ring. The bands between 1000 and 1350 cm^{-1} are assigned to the vibrations of C-O bonds. **(Liou T-H., 2010)**

A decrease in the intensity of the bands located at 1600 and 1100 cm^{-1} of synthesized material is observed. The appearance of an intense peak at 1250 cm^{-1} for materials thermally and chemically activated with $ZnCl_2$ is due to the presence of Zn. **(Spagnoli A.A et al., 2017)**
The band at 1641 cm^{-1} is pronounced for our impregnated activated material, and is associated with the aromatic stretching mode enhanced by the presence of polar groups. **(Fuente E et al., 2003)** Similarly, the small band at 1250 cm^{-1} is related to the C-O stretching of aromatic rings polarized by oxygen atoms bonded close to the carbon atoms **(Njoku V.O et al., 2011)**. Finally, a broad band between 1300 and 1040 cm^{-1} is attributed to C=O stretching in alcohols **(Zawadzki J, 1989)**, which appears to be most pronounced for CN carbons.

2.2.2 SEM characterization

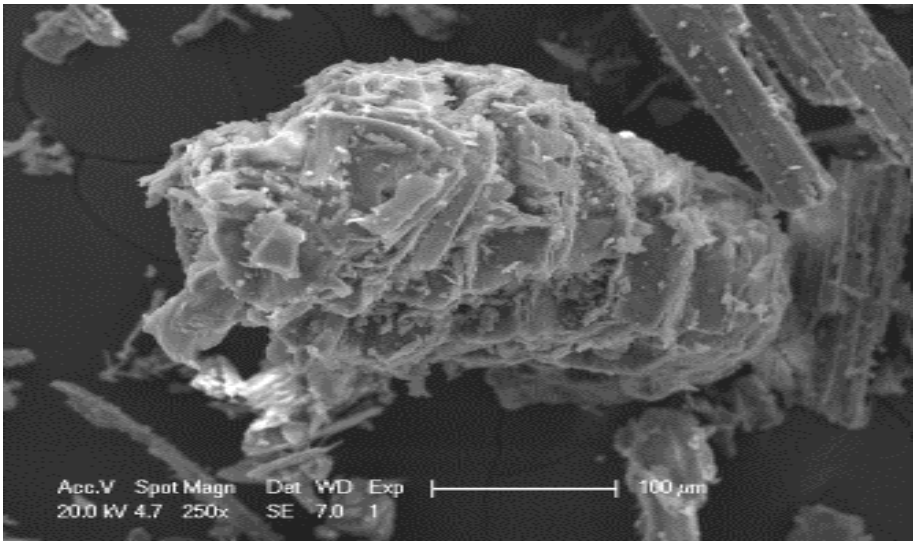

Fig.3 ***SEM photographs of the MRA***

Furthermore, activated carbons exhibit a uniform, highly porous, and well-pronounced range of porous structures, indicating a good opportunity for dyes to be trapped and adsorbed . It can be seen from the SEM images that the outer surface of the activated carbons was full of cavities. It appears that the cavities on the surface of the carbons result from the evaporation of $ZnCl_2$ during carbonization, leaving the space previously occupied by $ZnCl_2$ **(Chergui Y et al., 2019)**
Therefore, $ZnCl_2$ is an effective activating agent to obtain activated carbon with high specific surface area.

2.2.3 Effect of Adsorbent Mass

The experiments involved stirring 50 ml of a Rhodamine B solution with a concentration of 50 mg/L and a pH of 3, using various masses of chemically activated and thermally treated Grape Marc (**MRA**) in 250 ml beakers. Stirring was maintained for 120 minutes at a speed of 300 rpm and at room temperature. Subsequently, the suspensions were separated by centrifugation at 8000 rpm for 10 minutes. The filtrate containing the residual concentrations of Rhodamine B dye was then analyzed at 554 nm using a UV-visible spectrophotometer (Agilent Technologies Cary 60) at the appropriate wavelength (λmax = 554 nm).

2.2.4 Effect of Stirring Speed

Given the significant role of stirring speed in the adsorption phenomenon, the optimization of this parameter was pursued by introducing 1g masses of **MRA** into volumes (50 ml) of Rhodamine B solution with an initial concentration of 50 mg/L and stirring at different speeds (300; 600; 900; 1200; and 1500 rpm) for 120 minutes. Following agitation, the residual pollutant solution is separated by centrifugation at 8000 rpm for 10 minutes, and the supernatant is retrieved to measure its absorbance and subsequently analyzed at 554 nm.

2.2.5 pH Effect

The pH effect was investigated using a HANNA HI 3220 pH meter. Equal masses of 2 g of **MRA** were mixed with 50 ml volumes of Rhodamine B solutions at 50 mg/L in 50 ml beakers. The pH of the solutions was adjusted to the following values: 1, 2, 3, 4, 5, 6, 7, 8, 9, 10, 11, and 12 by adding either a few drops of concentrated HCl or NaOH 0.1 N solutions. The mixtures were then stirred at 1500 rpm for 120 minutes at room temperature. After the contact time, the material was separated by centrifugation for 10 minutes at 8000 rpm. The residual concentrations of the dye were determined using UV-Visible spectrophotometry at a wavelength of λ = 554 nm.

2.2.6 Effect of Initial Adsorbate Concentration

To study the effect of initial concentration, a mass of 0.7 g of **MRA** was mixed with Rhodamine B solutions of various concentrations (20; 25; 30; 40; 50; 60; 70; 80; and 90 mg/L) in 50 ml volumes. The mixture was stirred at a speed of 500 rpm for 120 minutes. Adsorption was carried out at a pH of 3 and at room temperature. The separation was performed by centrifugation at 8000 rpm for 10 minutes. The residual concentrations were determined using a UV-Vis spectrophotometer at 554 nm.

2.2.7 Adsorption Kinetics

Kinetic experiments involved mixing 50 ml solutions containing an initial Rhodamine B of 50 mg/l at pH 3 with one g masses of the **MRA** material in 250 ml beakers at room temperature. Homogenization of the mixtures was achieved using a magnetic stirrer at a constant speed of 1500 rpm. Samples were collected at various time intervals, and after separation of adsorbent/adsorbate, the dye concentration was determined via UV-Visible spectrophotometry at a wavelength of λ = 554 nm.

3. RESULTS AND DISCUSSION

3.1 Effect of Adsorbent Mass

The influence of the adsorbent mass was studied in the range of 0.006 - 2 g. The curve in Fig.4 shows that a mass of 1 g of **MRA** is capable of adsorbing a maximum of approximately 99% of the dye. The quantities of adsorbed dye should be in accordance with the doses of adsorbent in solution to ensure an equivalent number of adsorption sites. Beyond a certain mass, the highest value is 1 g, and then it stabilizes. This is easily understandable because increasing the mass of the adsorbent increases the number of available adsorption sites for the fixation of the adsorbed dye, thus favoring the decolorization phenomenon (**Makhlouf M et al., 2013**).

Therefore, it is useful to work with adsorbent doses $\leq$ 1 g and avoid ineffective overdosing. In the subsequent work and to determine the adsorption capacities by saturating all probable sites, it was chosen to work with adsorbent masses of 1 g.

Various results were obtained for the adsorption of methylene blue (MB) by activated olive kernels (AOK) (**Aziz A et al., 2009**). The highest value is 0.05 g, and then it stabilizes.

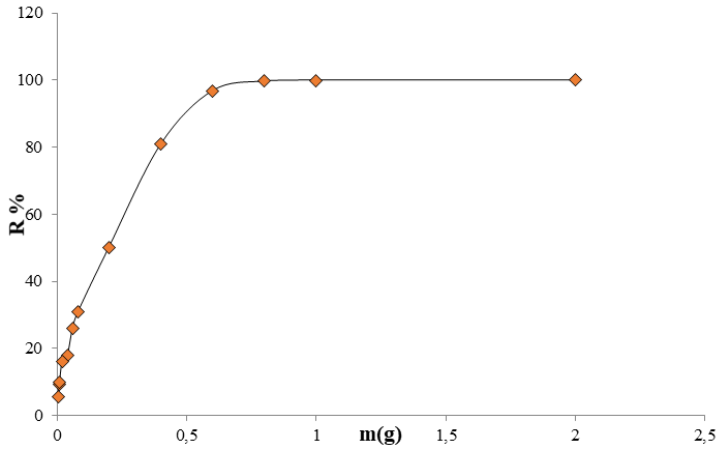

Fig.4 effect of adsorbent mass on Rhodamine B dye removal

3.2 Effect of Stirring Speed

The results depicted in Fig.5 show a decrease in adsorption capacity with increasing stirring speed up to 900 rpm. Beyond 900 rpm, the adsorption capacity increases with the increase in stirring speed, up to 1500 rpm, which is the optimal value.

There is considered to be an optimal stirring speed sufficient to enhance the contact between **MRA** molecules and Rhodamine B dye molecules and yet low enough to avoid disrupting the adsorption forces.

The same result was obtained with the malachite green (MG) dye by adsorption with agricultural waste potato peels (APP) (**Davydov L et al., 2001**), where the optimal value is 1500 rpm.

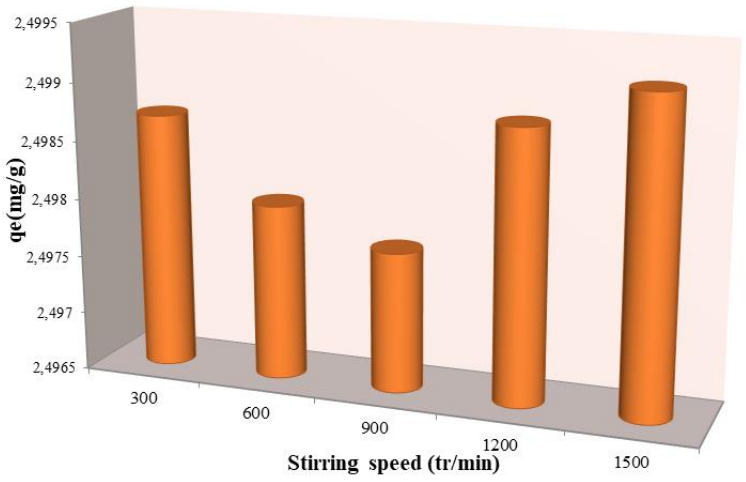

Fig.5 effect of stirring speed

3.3 pH Effect

The influence of the initial pH of the solutions in Fig.6 on adsorption was studied within the pH range of 1 to 12 and at different temperatures (30, 40, and 50 °C). The quantities of dye retained by the adsorbent from various solutions were found to be closely related to the initial pH value of the solution (Fig.6). The results obtained show that the variation in residual concentrations of Rhodamine B dye

is relatively small at 30 °C. However, for yields at temperatures of 40 and 50 °C, they decrease with increasing pH, reaching a maximum (99.92% and 99.80%) in an acidic environment (pH 4 and 3) respectively. Therefore, decolorization is minimally influenced by pH variation, and retention rates are significant for all pH values. Based on these results, all decolorization tests on MRA were conducted at the natural pH of the colored solution for the dye studied at 30°C, pH 4 for decolorization tests at 40°C, and pH 3 at T= 50°C.

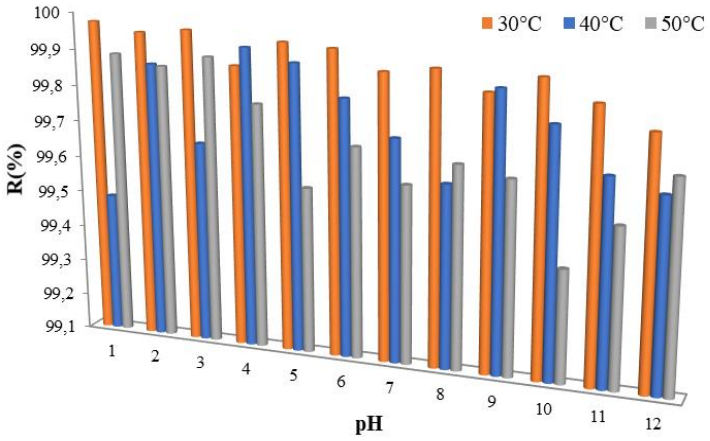

Fig.6 pH effect

3.4 Effect of Initial Adsorbate Concentration

The experiments were conducted within an initial Rhodamine B concentration range of 22 to 95 mg/L. The results obtained are illustrated by the curve in Fig.7.

According to the results, the adsorption capacity of **MRA** increases with the increase in initial dye concentrations, and there is no plateau within the studied concentration range. The highest studied value is 90 mg/l. This indicates that the saturation level has not been reached and that the material could adsorb larger amounts of dye. It would have been necessary to increase the dye concentration to determine the saturation threshold. Therefore, we chose to work at a concentration of 50 mg/L.

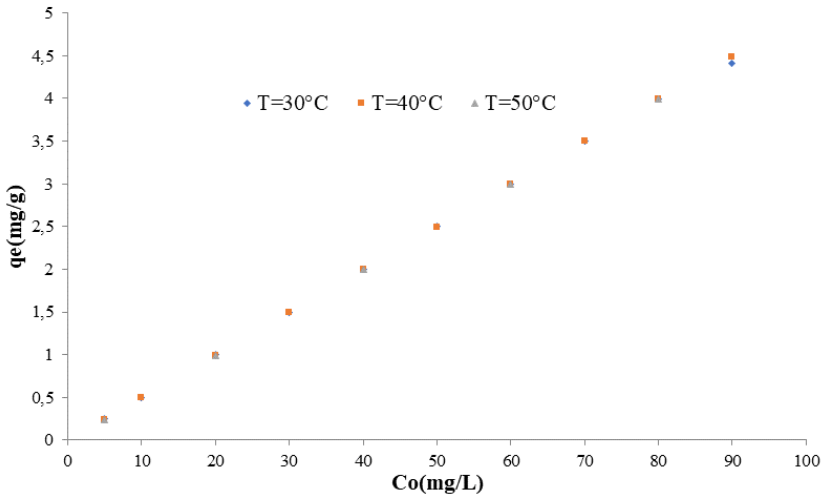

Fig.7 ***Effect of Initial Adsorbate Concentration***

3.5 Adsorption Kinetics

Fig.8 illustrates the effect of the initial molarity of Rhodamine B on the retention rate at different contact times.

The kinetic study of Rhodamine B dye removal by the material (**MRA**) demonstrates the effect of initial dye concentration on the retention rate at various contact times. For the three temperatures used, the retention rate increases with increasing reaction time, following two different slopes. The first slope is rapid and occurs within the first 10 minutes, while the second slope is slower and could indicate the equilibrium between retained and desorbed dye fractions. Overall retention is comparable for all three temperatures, with efficiency increasing as concentration increases, with magnitudes of 92%, 98%, and 95% respectively for temperatures of 30, 40, and 50°C. Most of the dye transferred to the adsorbent is obtained within the first 5 minutes, with considerable amounts for all three temperatures for the material with Rhodamine B dye.

The capacity of adsorption dye also increases with increasing solution dose, reaching values of approximately 1.94 mg/g, 2.2 mg/g, and 2.6 mg/g respectively for temperatures of 30, 40, and 50°C for the **MRA** material with Rhodamine B dye. The kinetic study of Rhodamine B dye removal by the adsorbent material (**MRA**) shows a decrease in residual concentration with increasing contact time at different temperature values. Indeed, the Rhodamin B dye first adsorbs on easily accessible sites, with diffusion towards adsorption sites of reduced accessibility occurring gradually during agitation until reaching adsorption equilibrium (**Chergui Y et al., 2018**). As observed in the study of the mass effect, it is also noted that the adsorption affinity of MRA is greater for the cationic dye Rhodamine B than for the anionic dye red bemacide RB-ETL (**Ouazani F et al., 2022**). After 60 minutes of contact, the decoloration efficiency of the Rhodamine B solution reaches 99.9% when using MRA. However, this efficiency does not exceed 85% in the case of red bemacide RB-ETL (**Sych NV et al., 2012**).

The reaction order is a very important parameter in determining reaction mechanisms. The orders for adsorption on biomasses most cited in the literature are:

1. The pseudo-first order expressed by the Lagergren equation. (Lagergren S., 1898)

$$\frac{dq_t}{dt} = K_1(q_e - q_t) \qquad (1)$$

After integrating between t = 0 and t, on one hand, and qt = 0, the equation becomes

$$Ln(q_e - q_t) = Lnq_e - K_1 t \qquad (2)$$

Where q(t): is the quantity of solute adsorbed at time t, qe is the quantity of solute adsorbed at equilibrium, and k1 is a kinetic constant (min^{-1})

2. The pseudo-second order expressed by the equation of HO and MCKAY. (Ho YS et al., 1999)

$$\frac{dq_t}{dt} = K_2(q_e - q_t)^2 \qquad (3)$$

After integration between t = 0 and t, on one hand, and q_t = 0 and q_t, we obtain the linear form:

$$\frac{t}{q_t} = \frac{1}{K_2 q_e^{\,2}} + \frac{1}{q_e} t \qquad (4)$$

Where k_2 is a kinetic constant ($g*mg^{-1}*min^{-1}$).

3. Elovich Model (Aharoni C et al., 1970), expressed by the following equation:

$$q_t = \left(\frac{1}{\beta}\right) Ln\ \alpha.\beta + \left(\frac{1}{\beta}\right) Ln\ t \qquad (5)$$

Where : α [mg*g^{-1}*min^{-1}] : Initial adsorption rate, β [mg*g^{-1}] : Constant related to the surface and the activation energy of chemisorption.

This model does not provide obvious assumptions for the retention mechanism. Nevertheless, it is recommended for highly heterogeneous systems.

4. Intraparticle diffusion expressed by the Weber and Morris equation (Weber WJ et al., 1963):

$$q_t = K_{int}\ .\ t^{\frac{1}{2}} \qquad (6)$$

Where K_{int} is the constant of intraparticle diffusion in (mg/g min$^{0.5}$), it depends on the diffusion coefficient of the species considered, as well as the pore size.

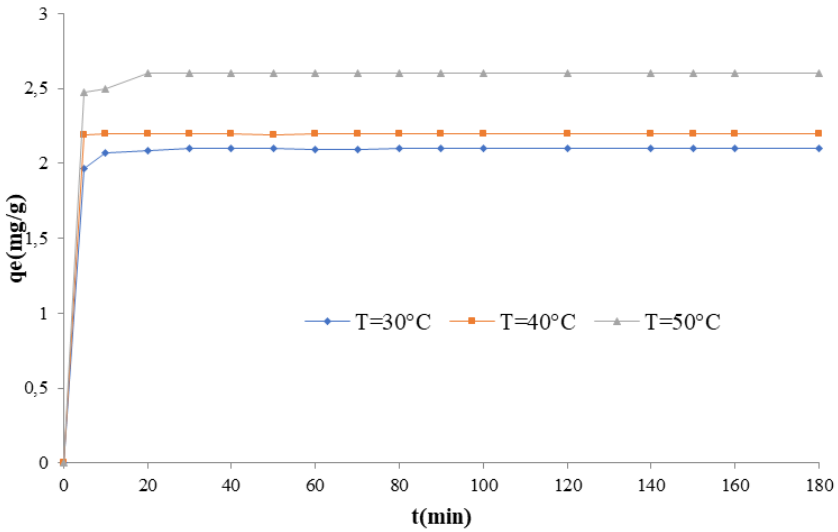

Fig.8 contact time effect on Rhodamine B removal

3.3.1 Kinetics of pseudo-first order

The constants of the pseudo-first order were determined by extrapolating the plot of ln(qe-qt) as a function of time. The value of the adsorbed quantity (qe), the pseudo-first order constants k_1, and the regression coefficients R^2 for the MRA material used are given in Table 1. The value of R^2 was found near from unity at different temperatures and equal to 0.96 and 0.97. The calculation of qe shows that the theoretical adsorption quantity is rather low compared to the experimental quantity. These observations lead us to say that the adsorption of the dye Rhodamine B does not express a process of controlled diffusion since it does not follow the equation of pseudo-first order, given by Lagergren.

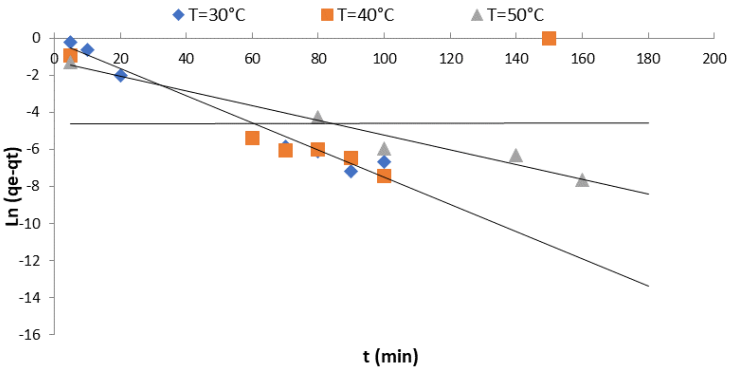

Fig.9 ***Pseudo-first order model***

3.3.2 Pseudo-second Order Kinetics

Fig.10 illustrates the application of the pseudo-second order kinetic model to the results obtained for Rhodamine B adsorption. The values of the adsorbed quantity (qe), pseudo-second order constants k_2, and regression coefficient R^2 utilized are provided in **Table.1**. Based on these results, it appears that the adsorbed quantity at equilibrium, qe, increases with increasing initial concentration, while the constant k_2 decreases. Moreover, the R^2 value is very high and exceeds 0.99 at different temperatures, far surpassing that obtained with the pseudo-first order model. The theoretical maximum adsorption quantities at equilibrium (qe) are approximately 2.01, 2.5, and 2.502, respectively, and they are very close to the experimentally found values (2.04, 2.29, 2.699 mg/g). These latter observations lead us to believe that the adsorption process follows the pseudo-second order model.

Thus, the adsorbed quantity at equilibrium depends solely on the initial dye concentration and the applied time, as reported by some authors (**Ho YS et al., 1999**).

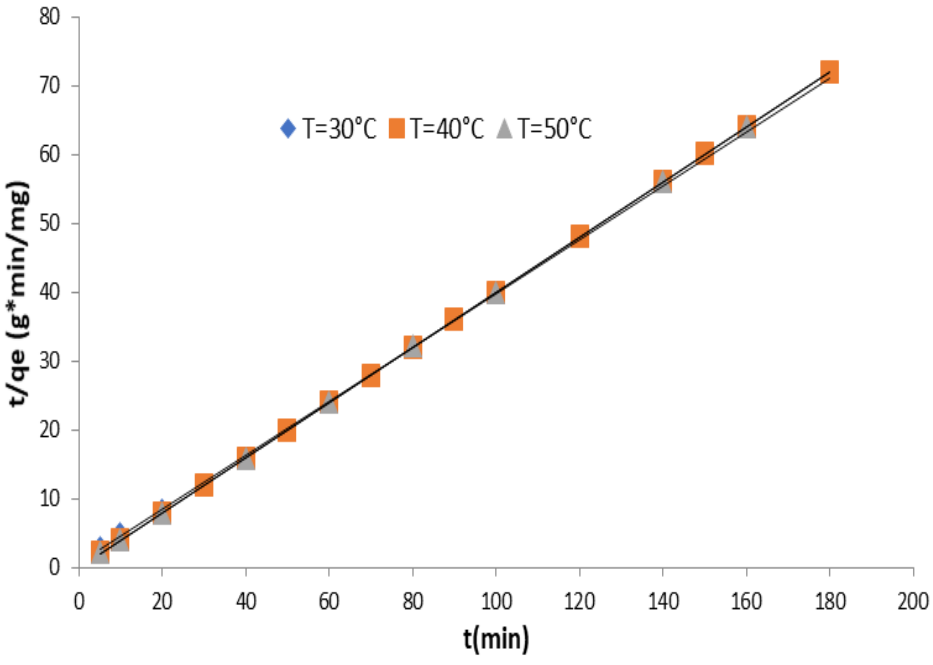

Fig.10 ***Pseudo-second Ordermodel***

3.3.3 Elovich Model

Plotting qt against ln t should yield a linear relationship with a slope of (1/β) and an intercept of (1/β) ln (αβ). Based on the correlation coefficient value, the kinetic data are better represented by the second-order kinetic model.

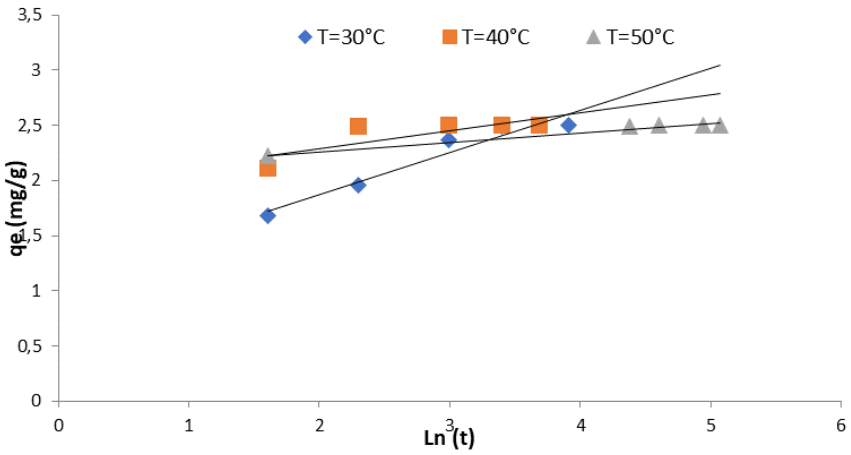

Fig.11 ***Elovich Model***

3.3.4 Diffusion Process

Fig.12 presents plots of intraparticle model for Rhodamine B dye removal. The value of the external diffusion constant, k_{id}, as well as that of R^2, are provided in **Table.1**. From this Fig, it is evident that intraparticle diffusion is a significant step in the adsorption process of basic dye (Rhodamine B) on MRA material, especially after the first 60 minutes. This latency period can be explained by the movement of dye molecules within the channels of the cellulose fiber adsorbent, before reaching the surface where they will be arranged in layers along the fibers. However, the surface chemical reaction, which begins within the first minutes of contact and whose experimental points align with the pseudo-second order with very high regression coefficients R^2, indicates that the most influential step in dye adsorption on MRA remains the intraparticle diffusion process, as it can be considered a limiting step controlling the dye transfer rate at each instant t.

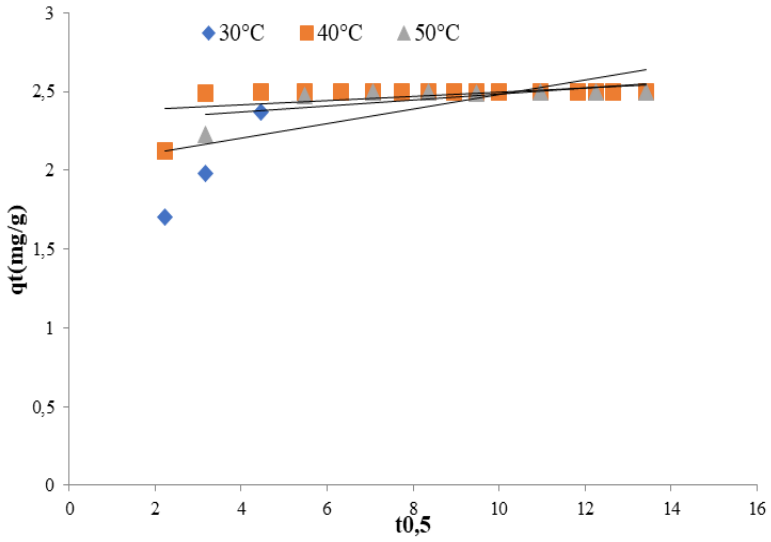

Fig.12 Intraparticle diffusion model

Table.1 Kinetic Parameters

	Matériau MRA		
Température	**30°C**	**40°C**	**50°C**
qe_{exp}	2,048	2,29	2,699
Modèle de Pseudo-first-order			
qe_{cal}	0,854	0,404	0,288
K_1	-0,073	-0,066	-0,039
R^2	0,971	0,967	0,964
Modèle de Pseudo-second-order			
qe_{cal}	2,015	2,500	2,502
K_2	0,152	0,159	0,159
R^2	0,999	1	1
Modèle d' Elovich			
β	2,625	1,576	11,904
α	7,065	13,969	$5,638*10^9$
R^2	0,943	0,634	0,975
Modèle de Diffusion intraparticullaire			
K_{id}	0,256	0,0008	0,132
C	1,141	2,488	1,817
R^2	0,974	0,99	0,939

3.5 Adsorption Isotherms

Fig.13 presents the equilibrium adsorbed quantities of dye (qe) as a function of equilibrium dye concentration at different temperatures. The illustration of the adsorption curves clearly shows that the isotherms of the three temperature values belong to the L type according to the classification of equilibrium isotherms in solution by Giles et al. (**Giles CH et al., 1960**). According to the literature, the experimental results of adsorption isotherms are described by different mathematical models. Models often used to fit equilibrium data are: Langmuir I, Langmuir II, Freundlich, and Temkin models, which are given by the following equations:

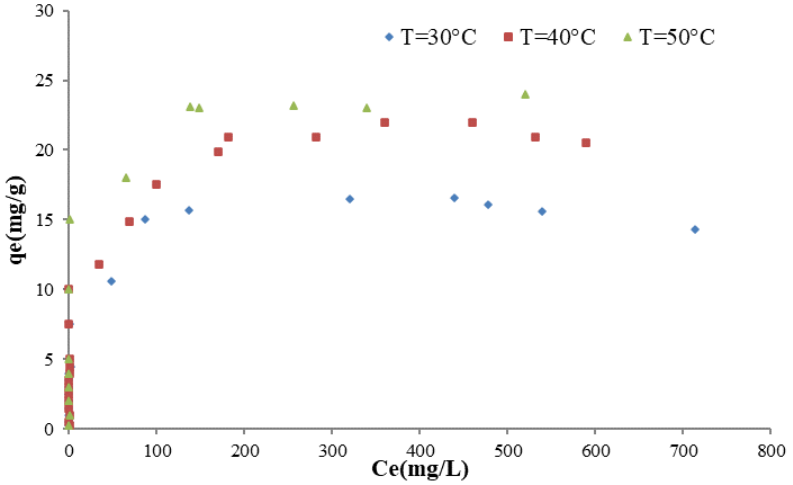

Fig.13 adsorption isotherm

3.5.1 Langmuir Model: (Langmuir I., 1916)

Commonly used equations:

$$\frac{1}{q_e} = \frac{1}{q_m} + \frac{1}{K_L\, C_e\; q_m} \qquad Langmuir\ I \qquad (7)$$

$$\frac{C_e}{q_e} = \frac{C_e}{q_m} + \frac{1}{K_L\, q_m} \qquad Langmuir\ II \qquad (8)$$

When qe and qm are expressed in mg/g and Ce in mg/L, the constant KL is expressed in L/mg. It should be noted that K_L is often referred to as b or L. Where: qe: equilibrium adsorption capacity (mg/g); qm: saturation adsorption capacity (mg/g); K_L: Langmuir constant (L/mg). The plot of Ce/qe vs. Ce allows for determining qm and KL.

3.5.2 Freundlich Model: (Freundlich HM., 1906)

The most common form is the logarithmic scale plot of qe variations as a function of Ce:

$$q_e = K_f C^{\frac{1}{n}} \qquad (9)$$

$$Lnq_e = LnK_f + \frac{1}{n}\,.Ln(C_e) \qquad (10)$$

Where: qe: equilibrium adsorption capacity (mg/g); n, Kf: Freundlich constants. The plot of log qe vs. log Ce allows for determining n and Kf.

3.5.3 Temkin Model: (Temkin MJ et al., 1940)

The linearized form of Temkin Equation is as follows: $q_e = \frac{R.T.q_m}{\Delta Q} LnK_T + \frac{R.T.q_m}{\Delta Q} LnC_e$ (11)

Where R = 8.314 J/mol·K, T: absolute temperature (in K), ΔQ: adsorption energy variation (in J/mol), and K_T: Temkin constant (in L/mg).

Table. 2 presents the values of Langmuir I, Langmuir II, Freundlich, and Temkin constants, extrapoated from the equations of these models. By fitting the experimental points to both models and based on the R^2 coefficient values, it appears that Langmuir II better expresses the adsorption type (R^2 close to unity). This adequacy is supported by the good correlation between (qexp) and (qcal). On the other hand, the negative constants of Langmuir I model imply its inadequacy in describing the experimental data.

Thus, dye molecules could be adsorbed in monolayers, without dye-dye interactions **(Hameed BH et al., 2008**). This hypothesis is reinforced by thermodynamic results indicating that the order increases during adsorption to ultimately provide a well-organized distribution of dye molecules at the adsorption sites.

The Freundlich model is characterized by the adsorption intensity (n), which indicates the magnitude and diversity of energies associated with a particular type of adsorption, while KF indicates the adsorption capacity. According to Weber et al., (**Weber WJ et al., 1992**), the higher the value of KF, the greater the affinity of the adsorbent for the adsorbate, and the more porous the adsorbent. Experimental results of the constants n are: 5.175, 4.572, and 5.602 for the material (MRA) at different temperatures (30, 40, and 50°C respectively). Furthermore, studies have shown that as the value of n approaches unity, the surface becomes more homogeneous. Considering the regression

coefficients obtained, which are close to unity for the material with Rhodamine B dye, it can be said that the adsorption of the dye used by the studied material is better described by the Freundlich model. Modeling the adsorption isotherms of Rhodamine B dye by the Temkin model can be applied to determine the variation in adsorption energy. According to the obtained results (**Table.2**), the values of adsorption energy variations are high and positive (ΔQ>0), and we judged that the tested model presents a good correlation (R^2 = 0.99).

Table.2 Isotherm parameters

	Material (MRA)		
T (°C)	**30°C**	**40°C**	**50°C**
$\mathbf{qe_{exp}}$	14,29	20,52	23,97
Langmuir I			
$\mathbf{q_m}$	8,532	16,920	21,231
$\mathbf{K_L}$	78,133	3,265	4,855
$\mathbf{R^2}$	0,897	0,925	0,872
Langmuir II			
$\mathbf{q_m}$	10,010	16,694	18,656
$\mathbf{K_L}$	0,382	0,394	1,142
$\mathbf{R^2}$	0,993	0,992	0,996
Freundlich			
n	5,175	4,572	5,602
$\mathbf{K_F}$	3,763	6,059	7,979
$\mathbf{R^2}$	0,992	0,993	0,993
Temkin			
B	0,766	2,170	1,687
$\mathbf{K_T}$	3920,863	48,408	269,395
ΔQ	32894,125	20019,249	29700,134
$\mathbf{R^2}$	0,990	0,990	0,993

3.4 Thermodynamic Temperature Effect

Fig.14 illustrates the influence of temperature on the dye retention rate on the adsorbent. From the Fig.14, it is observed that this rate decreases with increasing reactor temperature. This phenomenon, in accordance with the Arrhenius law, suggests that the surface reaction is exothermic, and that each increase in temperature unfavorably affects its progression.

Thermodynamic parameters such as standard Gibbs free energy (ΔG°), standard enthalpy (ΔH°), and standard entropy (ΔS°) have been determined using the following equations: (**Sawalha FM et al., 2007**)

$$K_d = \frac{C_e}{C_0 - C_e} \qquad (12)$$

$$\Delta G = \Delta G^0 - RT.LnK_d \qquad (13)$$

$$LnK_d = \left(\frac{\Delta S^0}{R}\right) - \left(\frac{\Delta H^0}{R}\right)\frac{1}{T} \qquad (14)$$

Where K_d is the distribution constant; R is the ideal gas constant [$J \cdot mol^{-1} \cdot K^{-1}$]; T is the absolute temperature [K].

Based on the obtained results (**Table.3**), it is observed that the free energy is negative in our case. This indicates that the adsorption of Rhodamine B on the MRA material is favorable, spontaneous, and reversible process (**Ouazani F et al., 2017**). Regardless of the temperature, the adsorption process of Rhodamine B dye on our support is physisorption since the values of ΔH° are below 40 KJ/mol **(Zayed AM et al., 2023**). The positive value of the standard entropy ΔS° indicates that the system transitions from a disordered state to a more ordered state. The negative free enthalpy implies that the adsorption process is exothermic. (**Zayed AM et al., 2023**).

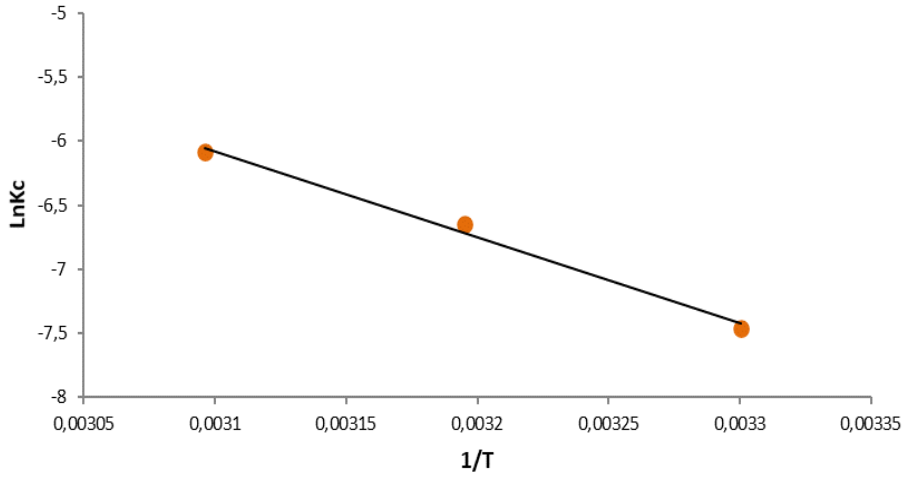

Fig.14 plot of LnKc Vs 1/T

Table.3 Thermodynamic parameters

Temperature(K°)	ΔH° (J/mol)	ΔS° (J/mol*K)	ΔG° (J/mol)	R^2
303	-55983,9818	123,030572	-93262,245	0,991
313			-94492,550	
323			-95722,856	

4. CONCLUSION

The study of the mechanisms of cationic dye Rhodamine B adsorption on MRA has been the focus of this work. The obtained results regarding kinetics, thermodynamics, and adsorption isotherms have been utilized to elucidate the dye fixation mode on the adsorbent. The investigation of the influence of initial concentration on kinetics revealed that the adsorption process follows the pseudo-second-order model. The adsorption capacity of an MRA mass increases with the rise in the initial concentration of the dye in the solution. Additionally, intraparticle diffusion appears to be a significant step in the adsorption process, particularly after the first 30 minutes of the reaction.

The positive values of both thermodynamic parameters indicate that the reaction is a spontaneous, endothermic chemisorption process, and the distribution order of dye molecules on MRA increases compared to that in the solution.

Reference

Aharoni C and Tompkins FC (1970). *Kinetics of adsorption and desorption and the Elovich equation. in: D.D. Eley, H. Pines, P.B. Weisz (Eds.), Advance in Catalysis and Related Subjects*. Academic Press, New York, USA, vol 21.

Aziz A, Elandaloussi E, Belhalfaoui B, Ouali MS, De Ménorval LC (2009). Efficiency of succinylated-olive stone biosorbent on the removal of cadmium ions from aqueous solutions. *Colloids and Surfaces B: Biointerfaces*, vol 73 pp 192-198.

Chergui Y, Iddou A, Hentit H, Aziz A, Jumas JC (2018). Biosorption of Textile Dye Red Bemacid ETL Using Activated Charcoal of Grape Marc (Oenological By-Product). *Key Engineering Materials*, vol 800 pp 151-156.

Choyk KH, Mckay G, Porter JF (1999). Sorption of acid dyes from effluents using activated carbon. *Resour Conserv Recycl*, vol 27 pp 57-71.

Djilani C, Zaghdoudi R, Modarressi A, Rogalski M, Djazi F (2012). «Elimination of organic micropollutants by adsorption on activated carbon prepared from agricultural waste». Chemical Engineering Journal. 189-190. 203-212.

Davydov L, Reddy EP, France P (2001). Smirniotis, Sonophotocatalytic destruction of organic contaminants in aqueous systems on TiO2 powders. *Applied Catalysis B: environmental*, vol 32 pp 95-105.

Faria PPC, Órfão JJM, Pereira MFR (2004). Adsorption of anionic and cationic dyes on activated carbons with different surface chemistries. *Water Research*, vol 38 pp 2043-2052.

Fuente E, Menéndez J.A, Díez M.A, Suárez D, Montes-Morán M.A (2003). «Infrared spectroscopy of carbon materials: a quantum chemical study of model compounds» The Journal of Physical Chemistry. B107. 6350–6359.

Freundlich HM (1906). Uber die adsorption in losungen. *Zeitschrift für Physikalische Chemie*, vol 57 pp 385-490.

Giles CH, MacEwan TH, Nakhwa SN, Smith D (1960). Studies in adsorption. Part XI. A system of classification of solution adsorption isotherms, and its use in diagnosis of adsorption mechanisms and in measurements of specific surface areas of solids. *Journal of the Chemical Society*, vol 10 pp 3973-3993.

Gomez V, Larrechi MS, Callao MP (2007). Kinetic and adsorption study of acid dye removal using activated carbon. *Chemosphere*, vol 69 pp 1151-1158.

Hameed BH, Mahmoud DK, Ahmad AL (2008). Equilibrium modeling and kinetic studies on the adsorption of basic dye by a low-cost adsorbent: coconut (*Cocos nucifera*) bunch waste. *Journal Hazardous Materials*, vol 158 pp 65-72.

Ho YS and Mc Kay G (1999). Pseudo-second order model for sorption processes. *Press Biochemistry*, vol 34 pp 451-465.

Kannan N and Sundaram MM (2002). Adsorption of congo red on various activated carbons. *Water Air Soil Pollution*, vol 138 pp 289-305.

Kennedy LJ, Vijaya JJ, Sekaran G, Kayalvizhi K (2007). Equilibrium, kinetic and thermodynamic studies on the adsorption of m-cresol onto micro- and mesoporous carbon. *Journal Hazardous Materials*, vol 149 pp 134-143.

Njoku V.O, Hameed B.H (2011). «Preparation and characterization of activated carbon from corncob by chemical activation with H3PO4 for 2, 4-dichlorophenoxyacetic acid adsorption». Chemical Engineering Journal. 173(2). 391–399.

Kushwaha A.K, Gupta N,. Chattopadhyaya M.C (2014). «Removal of cationic methylene blue and malachite green dyes from aqueous solution by waste materials of Daucus carota». Journal of Saudi Chemical Society 18(3). 200-207.

Lagergren S (1898). About the theory of so-called adsorption of soluble substances. *Kungliga Svenska Vetenskapsakademiens Handlingar*, vol 24 pp 1-39.

Langmuir I (1916). The constitution and fundamental propreties of solids and liquids. *Journal of the American Chemical Society*, vol 38 pp 2221-2295.

Liou T-H (2010). «Development of mesoporous structure and high adsorption capacity of biomass-based activated carbon by phosphoric acid and zinc chloride activation». Chemical Engineering Journal. 158. 129–142.

Makhlouf M, Hamacha R, Villières F, Bengueddach A (2013). Kinetics and thermodynamics adsorption of phenolic compounds on organic-inorganic hybrid mesoporous material. *International Journal of Innovation and Applied Studies*, vol 3 pp 1116-1124.

Mc Mullan G, Meehan C, Conneely A, Kirby N, Robinson T, Nigam P, Banat IM, Marchant R, Smyth WF (2001). Microbial decolourisation and degradation of textile Dyes. *Applied Microbiolgy Biotechnology*, vol 56 pp 81-87.

Ouazani F, Chergui Y, Benhammadi S, Saidi AFZ (2022). Three level design to estimate dyes adsorption parameters using oenological by-product as adsorbent. *Journal of Environmental Treatment Techniques*, Vol 10 pp 134-142.

Ouazani F, Iddou A, Aziz A (2017). Biosorption of bemacid red dye by brewery waste using single and poly-parametric study. *Desalination and Water Treatment*, pp 1-9.

Pearce CI, Lloyd JR, Guthrie JT (2003). The removal of colour from textilewastewater using whole bacterial cells. *Dyes Pigments*, vol 58 pp179-196.

Sawalha FM, Peralta-Videa JR, Romeo-Gonzalez J, Duarte-Gardea M, Gardea-Torresdey LJ (2007). Thermodunamic and isotherm studies of the biosorption of Cu(II), Pb(II) and Zn(II) by leavesof saltbush (Atriplex canescens. *Journal Chem Thermodynamics*, vol 39 pp 488-492.

Spagnoli A.A, Giannakoudakis D.A, Bashkova S (2017). «Adsorption of methylene blue on cashew nut shell based carbons activated with zinc chloride: The role of surface and structural parameters». Journal of Molecular Liquids 229. 465–471.

Sych NV, Trofymenko SI, Poddubnaya OI, Tsyba MM, Sapsay VI, Klymchuk DO, Puziy AM (2012). Porous structure and surface chemistry of phosphoric acid activated carbon from corncob. *Applied Surface Science*, vol 261 pp 75-82.

Temkin MJ, Pyzhev V (1940). Recent modifications to Langmuir isotherms. *Acta Physicochimica Sinica.U.R.S.S*, vol 12 pp 217-222.

Weber WJ, Mcginley PM, Katz LE (1992). «A distributed reactivity model for sorption by soils and sediments. Conceptual basis and equilibrium assessments». *Environmental Science and Technology*, vol 26 pp 1955-1962.

Weber WJ and Morris JC (1963). Kinetics of Adsorption on carbon from solution. *Journal of Sanitary Engineering*, vol 89 pp 31-60.

Zawadzki J (1989). «Infrared spectroscopy in surface chemistry of carbon, In: Thrower, P.A». Éd. Chemistry and Physics of Carbon, Marcel Dekker. New York. Basel. 21. 147–386

Zayed AM, Metwally BS, Masoud MA, Mubarak MF, Shendy H, Petrounias P, Abdel Wahed MSM (2023). Facile synthesis of eco-friendly activated carbon from leaves of sugar beet waste as a

superior nonconventional adsorbent for anionic and cationic dyes from aqueous solutions. *Arabian Journal of Chemistry*, vol 16 pp 1-19.